

Local probe of single phonon dynamics in warm ion crystals

A. Abdelrahman,^{1,2,*} O. Khosravani,¹ M. Gessner,^{3,4,5} A. Buchleitner,^{3,6} H.-P. Breuer,³ D. Gorman,¹ R. Masuda,¹ T. Pruttivarasin,^{1,7} M. Ramm,¹ P. Schindler,¹ and H. Häffner^{1,†}

¹*Department of Physics, University of California, Berkeley, California 94720, USA*

²*Department of Physics, Stanford University, 452 Lomita Mall, Stanford, CA 94305*

³*Physikalisches Institut, Albert-Ludwigs-Universität Freiburg,*

Hermann-Herder-Str. 3, D-79104 Freiburg, Germany

⁴*QSTAR, INO-CNR and LENS, Largo Enrico Fermi 2, I-50125 Firenze, Italy*

⁵*Istituto Nazionale di Ricerca Metrologica,*

Strada delle Cacce, 91, I-10135 Torino, Italy

⁶*Keble College, University of Oxford, OX1 3PG Oxford, United Kingdom*

⁷*Department of Physics, Mahidol University,*

272 Rama VI Rd., Ratchathewi, Bangkok 10400, Thailand

(Dated: November 9, 2021)

The detailed characterization of non-trivial coherence properties of composite quantum systems of increasing size is an indispensable prerequisite for scalable quantum computation, as well as for understanding of nonequilibrium many-body physics. Here we show how autocorrelation functions in an interacting system of phonons as well as the quantum discord between distinct degrees of freedoms can be extracted from a small controllable part of the system. As a benchmark, we show this in chains of up to 42 trapped ions, by tracing a single phonon excitation through interferometric measurements of only a single ion in the chain. We observe the spreading and partial refocusing of the excitation in the chain, even on a background of thermal excitations. We further show how this local observable reflects the dynamical evolution of quantum discord between the electronic state and the vibrational degrees of freedom of the probe ion.

Introduction

The faithful description of the state of an interacting many-particle quantum system turns ever more difficult as the system size increases¹⁻³. Therefore, one usually focuses on collective quantifiers – such as, e.g., the total magnetization of a spin chain – to distinguish macroscopically distinct many-body phases. However, engineered many-body quantum systems, such as trapped ions, cold atoms, and superconducting circuits, offer the unique and distinctive feature that their microscopic structure is accessible to experimental diagnostics⁵⁻¹³. Therefore, hitherto unaccessible dynamical features can be directly observed offering a novel opportunity to gain insight into the emergence of macroscopically robust features¹⁴⁻¹⁹. Further, the system size can be increased starting from only a few particles up to millions while maintaining coherent dynamics. Thus, those engineered systems allow one to study the emergence of macroscopic properties directly from the microscopic spectral and dynamical structure^{7,9}.

On the other hand, a microscopic approach where not only global observables but also the local ones as well as their correlations become an essential part of the description will at some point hit a complexity threshold. In particular, the increasing number of interacting degrees of freedom implies a rapidly proliferating number of possible defects, which induce disorder and/or noise; with finite temperature effects as one of the most fundamental and ubiquitous perturbations. Consequently, there is a conceptual and practical need to develop scalable and experimentally feasible approaches²⁰⁻²³ to probe well-defined microscopic quantum features such as correlation functions and quantum correlations even at system sizes which prevent an exhaustive microscopic characterization, and where the presence of uncontrolled noise such as a finite temperature is unavoidable. Such methods will help

to gain a better understanding of the ultimate realm of non-trivial quantum mechanical effects, on meso- and macroscopic scales. We believe that such methods could also be useful to characterize the naturally very complex functioning of quantum computing devices and thus help push quantum computing architectures to scales which become practically relevant.

To contribute to this endeavour, we present a tagging method which can be used to track single quantum excitations in warm quantum many-body systems. We achieve this by coupling an auxiliary qubit in form of the electronic state of a probe ion to the motion of an ion chain of variable length^{24–26}. We will demonstrate that this allows one to measure the autocorrelation function of the phonon dynamics even in situations where only access to a subsystem is available^{21,22}. Moreover, we will see that the local dynamics of the qubit is directly linked to the dynamical evolution of the quantum discord⁴ between the qubit degree-of-freedom of the probe ion and its local vibrational degree of freedom. We recall that discord describes local quantum properties of correlated states^{4,23} which are relevant for quantum information tasks such as entanglement distribution²⁷ and activation^{28,29}, as well as for local quantum phase estimation³⁰.

Results

Experimental system

The dynamics of the transverse motion (x, y) of an ion string aligned along the z -axis can be described by the Hamiltonian of a chain of coupled quantum harmonic oscillators^{31,32},

$$H_{\text{chain}} = \sum_{i=1}^N \hbar \omega_{x,i} a_i^\dagger a_i + \hbar \sum_{i=1}^N \sum_{\substack{j=1 \\ j < i}}^N t_{ij} (a_i^\dagger a_j + a_i a_j^\dagger), \quad (1)$$

where a_i is the annihilation operator acting on the Fock state of the i^{th} harmonic oscillator which represents the corresponding ion's transverse motional state, and the $\omega_{x,i}$ are the frequencies of the transverse motion of each ion along the k -vector of the qubit laser, which are modified by the Coulomb potential due to the interaction with neighboring ions. These frequencies are given by $\omega_{x,i} = \omega_x - \sum_{\substack{j=1 \\ j \neq i}}^N t_{ij}$ in which ω_x is the transverse trap center-of-mass frequency and t_{ij} is the coupling between the local modes of ions i and j ,

$$t_{ij} = \frac{1}{2} \frac{1}{m \omega_x} \frac{e^2}{4\pi \epsilon_0} \frac{1}{|z_i^0 - z_j^0|^3} \quad (2)$$

with the equilibrium position z_i^0 of the i th ion along the z axis.

We trap strings between eight and 42 $^{40}\text{Ca}^+$ -ions in a linear Paul trap (see Fig. 1) with trapping frequencies of $\omega_x = 2\pi \times \sim 1.9$ MHz, $\omega_y = 2\pi \times \sim 2.2$ MHz and ω_z ranging from $2\pi \times 94$ to $2\pi \times 196$ kHz.

The string is cooled by using laser light at 397 nm, red detuned with respect to the $S_{1/2} \leftrightarrow P_{1/2}$ transition, to the Doppler limit characterized by a mean phonon number $\bar{n} \approx 5$ of the transverse modes. To control the quantum information in the string, we drive the quadrupole transition between the $|S\rangle = |S_{1/2}, m_j = -1/2\rangle$ and $|D\rangle = |D_{5/2}, m_j = -1/2\rangle$ states by a 729 nm laser beam³³, as schematically shown in Fig. 1. This beam is tightly focused addressing the probe ion at the end of the ion chain, with a small projection on the z axis, and equal projections on the x and y axis. To create correlations between the electronic and motional degree of freedom, a short laser pulse $R^+(\theta, \varphi)$ with length θ and phase φ tuned to the $+\omega_x$ sideband of the quadrupole transition induces the coupling $|S, n\rangle \leftrightarrow |D, n+1\rangle$, where n labels a local motional Fock state of the addressed ion^{2,35}. To initially prepare a localized vibrational excitation, the pulse duration of 5 – 10 μs needs to be much shorter than the inverse coupling t_{12} of the local motion to the adjacent ion. Figure 2 shows a spectrum near the blue sideband of the x and y modes of a 42-ion string with axial frequency $\omega_z = 2\pi \times 72.14$ kHz. For long excitation times of 900 μs (red trace in Fig. 2), we resolve the normal modes of the 42 ion chain.

However, a short excitation time of 8 μs at about 250 times the intensity used to resolve the normal mode spectrum excites superpositions of the normal modes (blue trace in Fig. 2) corresponding to the desired local excitation of the ion string³².

After this initial state preparation, we allow the initially localized phonon to travel into the phonon bath of the warm ion string before a second probe pulse interrogates the coherence between the qubit and the vibrational motion (see Fig. 1)³⁶. Full interference contrast can only be restored if the original vibrational excitation refocuses at the probe ion simultaneously with the probe pulse. The observation of Ramsey fringes as a function of the relative phase between the two pulses can furthermore be traced back to qubit-phonon discord of the probe ion^{23,36} (see Supplementary Notes 1,2,3).

Theoretical interpretation

For the probe ion initially in the state $|S, n\rangle$, the preparation pulse $R^+(\theta, 0)$ of length θ and phase 0 creates a superposition of the form $\alpha_n |S, n\rangle + \beta_n |D, n+1\rangle$, where α_n and β_n are specific for each Fock state $|n\rangle$. The inverse operation can be applied with a second pulse, with the same parameters but opposite phase $\Delta\varphi = \pi$ with respect to the first pulse.

As long as the system has not evolved between both pulses, we expect full contrast. However, if the phonon created by the preparation pulse is no longer localized at the probe ion, the second pulse (see Fig. 1) cannot map the qubit-phonon coherences back to the electronic populations and therefore no phase dependency can be observed. Thus, loss of phase contrast indicates delocalization of the phonon excitation that is tagged by the probe ion's internal state (see Supplementary Notes 1,2,3 for

a detailed derivation).

More specifically, the phase contrast, or visibility

$$v(t) = \frac{\max_{\varphi}(P_D(t)) - \min_{\varphi}(P_D(t))}{\max_{\varphi}(P_D(t)) + \min_{\varphi}(P_D(t))}, \quad (3)$$

where P_D is the probability that after the Ramsey sequence with free evolution time t the ion is found in the excited $|D_{1/2}, m_j = -1/2\rangle$ state. The visibility $v(t)$ is closely connected to both the autocorrelation function of the probe ion's vibrational degree of freedom and to the discord between the electronic and the motional degrees of freedom of the probe ion (see Eqs. (19,29,32) of Supplementary Notes 1 and 3). The reason for this is that all three quantities relate to the coherences between the electronic states $|S\rangle$ and $|D\rangle$ in the density matrix pertaining to the motional degrees of freedom of the probe ion.

In order to make a quantitative connection, we assume that the density matrix describing the ion string after laser cooling is diagonal in the collective mode basis and that all modes are equally populated. This is justified by noting that laser cooling acts on the individual ions on time scales faster than the coupling between ions and that the spread of the eigenmode frequencies are nearly degenerate.

With these assumptions, we find in Supplementary Note 2 (see Eqs. 19,22 therein) for the modulus of the correlation function $|C(t)|$

$$|C(t)| = |\langle a_1(t)a_1^\dagger(0) \rangle| = (\bar{n} + 1)v(t), \quad (4)$$

where $\bar{n} = \langle a_i^\dagger a_i \rangle \approx 5$ is the average number of phonons in each of the normal modes. Further, we arrive at a simple measure for the quantum discord (Eq. 32 of Supplementary Note 3):

$$D(t) = \frac{\pi |C(t)|}{4\bar{n} + 1} = \frac{\pi}{4}v(t). \quad (5)$$

To derive this relation we have performed a perturbation expansion for small $\theta/2 \approx 0.3$, including contributions of first and second order, and used the additional assumption that the initial phonon state may be approximated by an equilibrium state of the local phonon modes (for details see Supplementary Note 3).

Experimental results

For the experiments, we first determine the time it takes to excite the probe ion to the $|D\rangle$ -level with a probability of 0.5, nearly saturating the transition for finite-temperature ion strings. We call this time the effective π -time t_π . The actual sequence to probe the dynamics of the crystal consists of two pulses each of length $t_\pi/2$ (see Fig. 1) and separated by time t . To detect and quantify the discord between qubit and local vibrational degree of freedom, we vary the phase difference $\Delta\varphi$ between the

first and the second Ramsey pulses. In particular, we choose $\Delta\varphi = \{0, \pi/2, \pi, 3\pi/2\}$ and extract the phase contrast $v(t)$ for each value of the free evolution time t . Figure 3 shows a comparison of the experimentally inferred phase contrast for 42 ions to the theoretical expectations as given by Eq. (19) in Supplementary Note 1.

To gather sufficient statistics, we repeat the experiment 500-750 times per data point. For short times t , we observe a large phase contrast as the phonon excitation is still localized at the site of the probe ion. After a few tens of microseconds, the phonon excitation couples to the other sites³² and the phase contrast diminishes. However, the phase contrast revives when the phonon excitation recurs at the original site. This revival of the phase contrast also proves that the phase coherence of the initially injected phonon is maintained even as it delocalizes over the ion string. We also study this dynamics for 8, 14, 25 and 33 ions (see Fig. 4).

Common to all measurements is a rapid loss of phase contrast followed by a specific revival pattern. Comparison with theory shows that the revival pattern is governed by the phonon dynamics in the ion chain. However, we also observe a reduction of the maximally expected visibility from 1 to values between 0.66 and 0.80. The reduction is independent of the Ramsey gap time, consistent with the measured Gaussian qubit decoherence with $T_2 \sim 2$ ms. Instead, we attribute the reduced contrast mainly to a broad incoherent background of the laser light (see Methods).

Discussion

We expect that suitable extensions of the scheme to protocols consisting of more than one ion or two pulses are in fact capable of extracting higher-order phonon correlation functions both in space and time. This way, the methods of non-linear spectroscopy, which are typically employed to study dynamical and spectral features of molecular aggregates and semiconductors³, become accessible to probe quantum optical many-body systems. This opens up a powerful way of analyzing complex interacting quantum systems by measuring space and time correlations^{21,22}

In this context, it is also interesting to note that the method tracks an excitation in a bath of substantial size. In the example of a 42-ion string cooled down to the Doppler limit of about five local transverse quanta, there are about $42 \times 5 \approx 200$ phonons present. Our method generates a single phonon and tags it with a specific phase relationship to the electronic state of the probe ion, allowing us to re-identify this excitation when it returns to its origin. Hence, the method allows to follow the dynamics of single phonons in a finite temperature environment.

Our measurements also show that quantum coherence of motional excitations can be preserved even in long ion strings. Direct extensions of this work are to measure how phonons scatter off im-

purities and how this affects the transport dynamics in a finite temperature environment³⁸. This could be done by coupling some of the phonons to individual qubits of other ions via sideband interactions. These interactions implement a non-linear dynamics in the photon bath allowing one to study more complex cases than the linear dynamics studied here. Further extensions include perturbing the potential with an optical lattice enabling studies of nanofriction and the Aubry-transition³⁹ or the interplay of disorder and interactions⁴⁰.

More generally, it would be interesting to study how this method could be applied to other systems, e.g., interacting spin chains, where individual excitations could be coherently traced via an auxiliary probe spin.

Finally, our method is scalable in the sense that the control of the subsystem is independent of the size of the total system. Thus, the discussed method can be applied or adapted to large coherent systems where suitable single particle control is available, such as for instance for neutral atoms in optical lattices⁶.

I. ACKNOWLEDGMENTS

This work has been supported by AFOSR through the ARO Grant No. FA9550-11-1-0318 and by the NSF CAREER programme grant no. PHY 0955650. A.B. & H.P.B. acknowledge support through the EU Collaborative Project QuProCS (Grant agreement 641277).

II. CONTRIBUTIONS

H.H., M.G., M.R., and T.P. conceived the experiment. A.A., M.R., T.P., R.M., D.G., and P.S. carried out the measurements. O.K., M.G., H.P.B., and A.B. carried out the theoretical analysis, A.A., H.H., O.K., M.G., H.P.B., and A.B. wrote the manuscript. All authors contributed to the discussions of the results and manuscript.

III. COMPETING FINANCIAL INTERESTS

The authors declare no competing financial interests.

* Corresponding author: mabd@kth.se

† Corresponding author: hhaeffner@berkeley.edu

- ¹ Chuang, I. L. and Nielsen, M. A. Prescription for experimental determination of the dynamics of a quantum black box. *J. Mod. Opt.* **44**, 2455 (1997).
- ² Häffner, H., *et al.* Scalable multiparticle entanglement of trapped ions. *Nature* **438**, 643–646 (2005).
- ³ Walschaers, M., Schlawin, F., Wellens, T., & Buchleitner, A. Quantum Transport on Disordered and Noisy Networks: An Interplay of Structural Complexity and Uncertainty. *Annual Review of Condensed Matter Physics* **7**, 223 (2016).
- ⁴ Modi, K., Brodutch, A., Cable, H., Paterek, T., & Vedral, V. The classical-quantum boundary for correlations: Discord and related measures. *Reviews of Modern Physics* **84**, 1655–1707 (2012).
- ⁵ Friedenauer, H., *et al.* Simulating a quantum magnet with trapped ions. *Nature Physics* **4**, 757–761 (2008).
- ⁶ Bakr, W., Gillen, J., Peng, A., Fölling, S., & Greiner, M. A quantum gas microscope for detecting single atoms in a Hubbard-regime optical lattice. *Nature* **462**, 74–77 (2009).
- ⁷ Senko, C., *et al.* Quantum simulation. Coherent imaging spectroscopy of a quantum many-body spin system. *Science (New York, N.Y.)* **345**, 430–3 (2014).
- ⁸ Hild, S., *et al.* Far-from-Equilibrium Spin Transport in Heisenberg Quantum Magnets. *Physical Review Letters* **113**, 147205 (2014).
- ⁹ Jurcevic, P., *et al.* Spectroscopy of Interacting Quasiparticles in Trapped Ions. *Physical Review Letters* **115**, 100501 (2015).
- ¹⁰ Langen, T., *et al.* Experimental observation of a generalized Gibbs ensemble. *Science (New York, N.Y.)* **348**, 207–11 (2015).
- ¹¹ Labuhn, H., *et al.* Tunable two-dimensional arrays of single Rydberg atoms for realizing quantum Ising models. *Nature* **534**, 667–670 (2016).
- ¹² Roushan, P., *et al.* Observation of topological transitions in interacting quantum circuits. *Nature* **514**, 241–244 (2014).
- ¹³ Hacoen-Gourgy, S., Ramasesh, V., De Grandi, C., Siddiqi, I., & Girvin, S. Cooling and Autonomous Feedback in a Bose-Hubbard Chain with Attractive Interactions. *Physical Review Letters* **115**, 240501 (2015).
- ¹⁴ Olkiewicz, R. and Garbaczewski, P. Dynamics of Dissipation. *Lecture Notes of Physics*, 597 (2002).
- ¹⁵ Buchleitner, A. & Kolovsky, A. Interaction-induced decoherence of atomic Bloch oscillations. *Physical Review Letters* **91**, 253002 (2003).
- ¹⁶ Amico, L., Osterloh, A. & Vedral, V. Entanglement in many-body systems. *Reviews of Modern Physics* **80**, 517–576 (2008).
- ¹⁷ Polkovnikov, A., Sengupta, K., Silva, A., & Vengalattore, M. Colloquium: Nonequilibrium dynamics of closed interacting quantum systems. *Reviews of Modern Physics* **83**, 863–883 (2011).

- ¹⁸ Geiger, T., Wellens, T. & Buchleitner, A. Inelastic Multiple Scattering of Interacting Bosons in Weak Random Potentials. *Physical Review Letters* **109**, 030601 (2012).
- ¹⁹ Gessner, M., Ramm, M., Häffner, H., Buchleitner, A. & Breuer, H. Observing a quantum phase transition by measuring a single spin. *Europhysics Letters* **107**, 40005 (2014).
- ²⁰ Knap, M., *et al.* Probing Real-Space and Time-Resolved Correlation Functions with Many-Body Ramsey Interferometry. *Physical Review Letters* **111**, 147205 (2013).
- ²¹ Gessner, M., Schlawin, F., Häffner, H., Mukamel, S. & Buchleitner, A. Nonlinear spectroscopy of controllable many-body quantum systems. *New Journal of Physics* **16** 092001 (2014).
- ²² Schlawin, F., Gessner, M., Mukamel, S. & Buchleitner, A. Nonlinear spectroscopy of trapped ions. *Physical Review A* **90**, 023603 (2014).
- ²³ Gessner, M., Breuer, H. & Buchleitner, A. The local detection method: Dynamical detection of quantum discord with local operations. *arXiv:1606.09049* [quant-ph] (2016).
- ²⁴ De Chiara, G., Calarco, T., Fishman, S. & Morigi, G. Ramsey interferometry with a spin embedded in a Coulomb chain. *Physical Review A* **78**, 043414 (2008).
- ²⁵ Baltrusch, J., Cormick, C. & Morigi, G. Quantum quenches of ion Coulomb crystals across structural instabilities. II. Thermal effects. *Physical Review A* **87**, 032116 (2013).
- ²⁶ Clos, G., Porras, D., Warring, U. & Schaetz, T. Time-resolved observation of thermalization in an isolated quantum system. *Physical Review Letter* **117**, 170401 (2016).
- ²⁷ Streltsov, A., Kampermann, H. & Bruß, D. Quantum cost for sending entanglement. *Physical Review Letters* **108**, 250501 (2012).
- ²⁸ Streltsov, A., Kampermann, H. & Bruß, D. Linking quantum discord to entanglement in a measurement. *Physical Review Letters* **106**, 160401 (2011).
- ²⁹ Piani, M., Gharibian, S., Adesso, G., Calsamiglia, J., Horodecki, P. & Winter, A. All nonclassical correlations can be activated into distillable entanglement. *Physical Review Letters* **106**, 220403 (2011).
- ³⁰ Girolami, D., *et al.* Quantum Discord Determines the Interferometric Power of Quantum States. *Physical Review Letters* **112**, 210401 (2014).
- ³¹ James, D. F. V. Quantum dynamics of cold trapped ions with application to quantum computation. *Applied Physics B: Lasers and Optics* **66**, 181–190 (1998).
- ³² Ramm, M., Pruttivarasin, T. & Häffner, H. Energy transport in trapped ion chains. *New Journal of Physics* **16**, 063062 (2014).
- ³³ Nägerl, H. C. *et al.* Investigating a qubit candidate: Spectroscopy on the $S_{1/2}$ to $D_{5/2}$ transition of a trapped calcium ion in a linear Paul trap. *Physical Review A* **61**, 23405 (2000).

- ³⁴ Leibfried, D., Blatt, R., Monroe, C. & Wineland, D. Quantum dynamics of single trapped ions. *Reviews of Modern Physics* **75**, 281–324 (2003).
- ³⁵ Wineland, D. *et al.* Experimental Issues in Coherent Quantum-State Manipulation of Trapped Atomic Ions. *Journal of Research of the National Institute for Standards and Technology* **103**:259–328, (1998).
- ³⁶ Gessner, M., *et al.* Local detection of quantum correlations with a single trapped ion. *Nature Physics* **10**, 105–109 (2013).
- ³⁷ Mukamel, S. Principles of Nonlinear Optics and Spectroscopy. *Oxford Univ. Press, New York* (1995).
- ³⁸ Cormick, C. & Schmiegelow, C. T. Noise-induced transport in the motion of trapped ions. *Physical Review A* **94**, 053406 (2016).
- ³⁹ Bylinskii, A., Gangloff, D. & Vuletić, V. Tuning friction atom-by-atom in an ion-crystal simulator. *Science* **348**, 1115–1118 (2015).
- ⁴⁰ Basko, D. M., Aleiner, I. L. & Altshuler, B. L. Metalinsulator transition in a weakly interacting many-electron system with localized single-particle states. *Annals of Physics* **321**, 1126–1205 (2006).

METHODS

Decoherence due to laser light

We observe a reduction of the maximally expected visibility from 1 to between 0.66 and 0.80. The reduced contrast is mainly due to a broad incoherent background on the laser light on the order of $B = -40$ dB below the carrier of the laser light, however, peaking to around $B = -28$ dB near the bandwidth of 700 kHz of our servo loop to stabilize the laser frequency. This incoherent background drives other transitions than the blue sideband, and in particular the strong atomic carrier transitions between the $S_{1/2}$ ($m_J = -1/2$) and $D_{5/2}$ ($m_J = \{-5/2, -3/2, -1/2, 1/2, 3/2\}$) levels. Our geometry was not optimized to drive only the $S_{1/2}$ ($m_J = -1/2$) and $D_{5/2}$ ($m_J = -1/2$) transition, and hence we assume that all carrier transitions have a similar coupling strength of $\Omega_0 \approx 150$ kHz when driving effective π -pulses on the blue sideband in $t_\pi = 20$ μ s. Thus, the population of the D-state will increase by $\sin(\sqrt{B}\Omega_0 t_\pi/2)$, corresponding to an increase between 0.016 ($B = -40$ dB) and 0.06 ($B = -28$ dB) for each $\pi_{\text{eff}}/2$ -pulse and transition. We estimate that this effect accounts for 0.2 of the loss of contrast for both pulses and all five atomic carrier transitions.

Another concern is motional heating during the free evolution time. In our trap, motional heating almost exclusively stems from voltage noise at the trap electrodes resulting in common noise to all ions. Thus, the center-of-mass mode heats with about 0.2 quanta / ms while all other modes heat with less than 0.01 quanta/ms. Because the heating is predominantly common mode, motional heating will not influence the intrinsic dynamics of the ion string.

DATA AVAILABILITY

All relevant data is available from the authors.

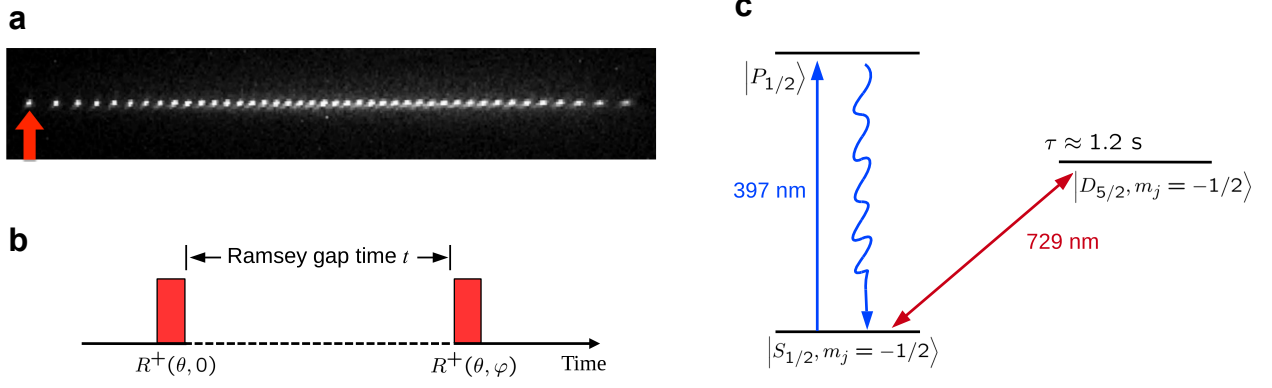


FIG. 1. **Schematic overview and electronic structure of $^{40}\text{Ca}^+$.** a, image of 42 ions. The red arrow indicates the position of the laser beam exciting the probe ion on the blue motional sidebands of the transverse motion with light at 729 nm. b, Ramsey sequence with a free evolution time t governed by the Coulomb interaction between the ions. c, relevant electronic levels of $^{40}\text{Ca}^+$. The quadrupole transition between the $|S_{1/2}, m_j = -1/2\rangle$ and $|D_{5/2}, m_j = -1/2\rangle$ states is driven by a narrow linewidth 729 nm laser beam tightly focused on the probe ion. The Zeeman degeneracy is lifted by applying a magnetic field of 323 μT . Cooling and readout are performed on the $|S_{1/2}\rangle \rightarrow |P_{1/2}\rangle$ transition at 397 nm.

SUPPLEMENTARY NOTE 1. RAMSEY SEQUENCE ON THE LOCAL SIDEBAND TRANSITION

The experimental sequence consists of two fast, focussed pulses, which are separated by free evolution, and each of which addressing the blue sideband transition of the outermost ion. The second local pulse is applied with a phase shift of π with respect to the first pulse. In the following we describe the elementary ingredients for the resulting Ramsey scheme.

A. Hamiltonian in the absence of laser pulses

In the absence of laser pulses, the ion chain is described by the Hamiltonian

$$H_{\text{free}} = \hbar\omega_0\sigma_+\sigma_- + H_{\text{ph}}, \quad (6)$$

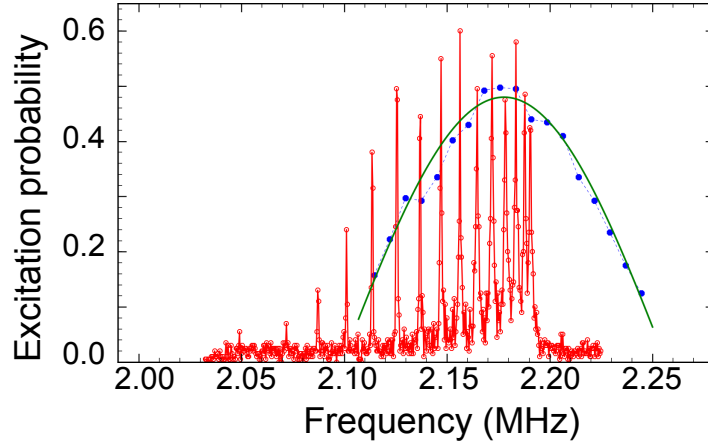


FIG. 2. **Spectra of blue transverse sidebands of a 42 ion string.** Excitation probability to the $|D_{1/2}, m_j = -1/2\rangle$ state of the probe ion as a function of the detuning. Red: excitation time of 900 μs , together with a relatively low intensity resolves individual normal modes. Visible are the normal modes of the x direction. Blue: a short high-intensity pulse of length 8 μs excites superpositions of the normal modes. Green: fit of the excitation to a sinc-function with only the amplitude and center frequency as free parameters.

where ω_0 is the electronic (carrier) transition frequency and $\sigma_+ = \sigma_-^\dagger = |D\rangle\langle S|$, with $|D\rangle$ and $|S\rangle$ denoting the electronic ground state D and excited state S of the outermost ion in the chain. Since other electronic levels as well as the electronic states of other ions are not populated in the course of the experimental sequence, they can be ignored in the theoretical description. The second term H_{ph} describes the motional states (phonons) of the chain as defined in Eq. (1) of the main manuscript. The phonon Hamiltonian H_{ph} is diagonalized in terms of annihilation operators A_j of the collective modes as

$$H_{\text{ph}} = \sum_j \hbar\omega_j A_j^\dagger A_j, \quad (7)$$

where ω_j is the frequency of the j th eigenmode. The basis transformation between collective phonon modes (A_j) and local modes (a_i) is described by a unitary matrix of coefficients β_{ij} , such that

$$a_i = \sum_{j=1}^N \beta_{ij} A_j. \quad (8)$$

B. Initial state

After Doppler cooling and optical pumping, the ion chain is initialized in the quantum state:

$$\rho_{\text{in}} = |S\rangle\langle S| \otimes \rho_{\text{ph}}, \quad (9)$$

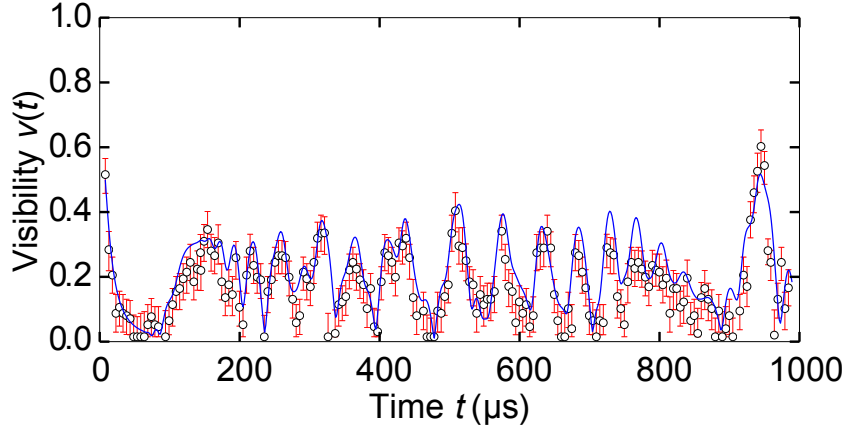


FIG. 3. **Visibility measurement for 42 ions.** Visibility (according to Eq. 3) deduced from the population evolution of the state $|D_{1/2}, m_j = -1/2\rangle$ as a function of the free evolution time t of the Ramsey sequence. A partial revival of the initial state population occurs at the rephasing times of the eigenfrequencies. Experimental results (red circles) are shown along with theory (blue line), for a chain of 42 ions with an axial trapping frequency $\omega_z = 2\pi \times 106.9$ kHz. Error bars represent the Bayesian 90% credible interval for the visibility. The only free parameter in the fit is an overall scale factor of the visibility of 0.67 to take into account loss of coherence mainly due to the incoherent background of the laser light (see text).

where $|S\rangle\langle S|$ denotes the electronic ground state of the first ion and ρ_{ph} represents a thermal state of motion, which is diagonal in the energy eigenbasis¹

$$\rho_{\text{ph}} = \frac{1}{Z_A} e^{-H_{\text{ph}}/k_{\text{B}}T}, \quad (10)$$

with $Z_A = \text{tr}(e^{-H_{\text{ph}}/k_{\text{B}}T})$, Boltzmann constant k_{B} and temperature T .

C. Sideband pulses

The Ramsey pulses in this experiment couple the electronic states of the first ion, $|S\rangle$ and $|D\rangle$, to its motional states via sideband transitions. In the experiment, both Ramsey pulses are focused on the same single ion, while being applied with a pulse duration of 5 – 13 μs , which leads to a spectral spread of $2\pi \times (69 - 178)$ kHz. In all of these experiments the spread of the eigenmodes that are involved in the motion of the first ion (with Lamb-Dicke factors of larger than 0.01) is less than $2\pi \times 58$ kHz. Therefore, the pulse occurs on a faster time-scale than the phonon tunneling, thereby creating localized phonons at the first ion. In a suitable interaction picture, this local sideband transition is therefore described by the Hamiltonian

$$H = \frac{\hbar\Omega_0}{2} \left(\sigma_+ e^{i(\mathbf{k}_L \cdot \mathbf{x}_1(t) - \Delta \cdot t + \phi)} + \sigma_- e^{-i(\mathbf{k}_L \cdot \mathbf{x}_1(t) - \Delta \cdot t + \phi)} \right), \quad (11)$$

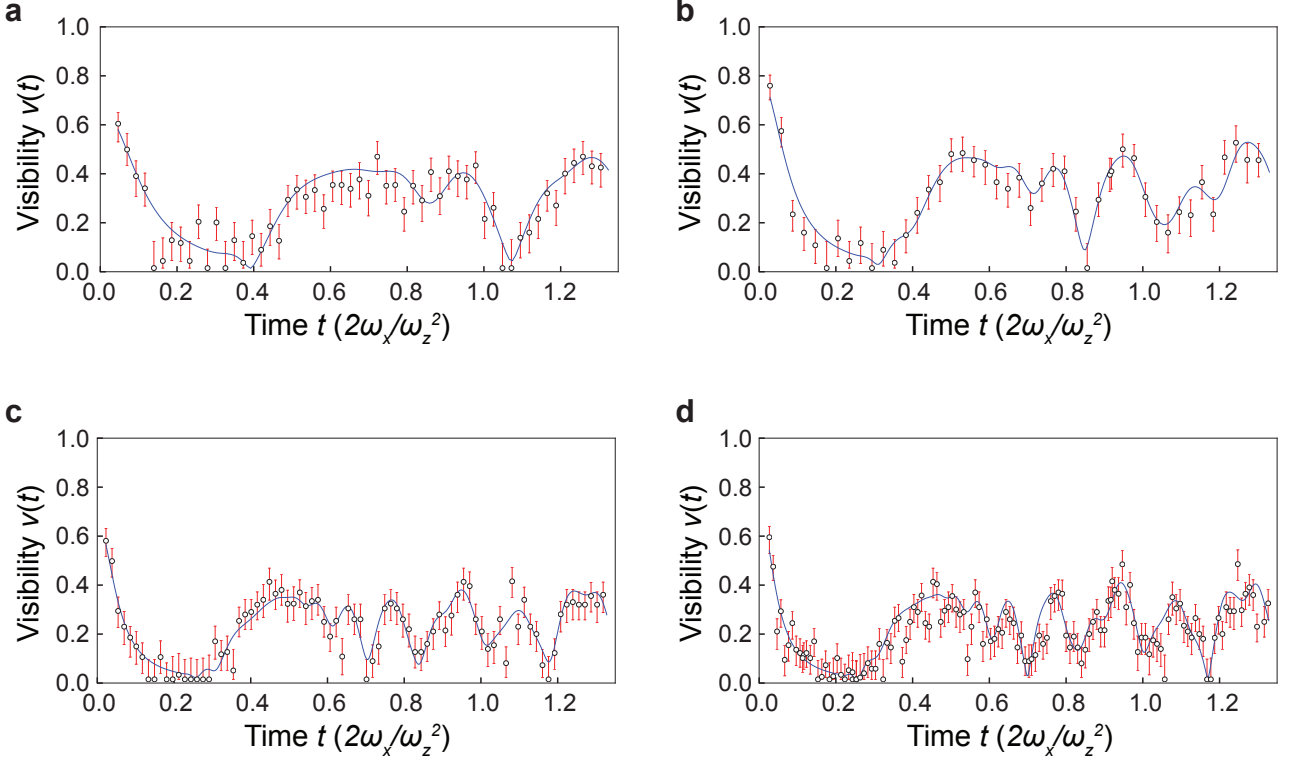


FIG. 4. **Visibility measurements for a variable number of ions.** Experimental result in **a**, is for 8 ions, **b**, 14 ions, **c**, 25 ions, and **d**, with 33 ions where the axial trapping frequency takes the values $\omega_z = 2\pi \times (195.8 \text{ kHz}, 155.2 \text{ kHz}, 93.8 \text{ kHz}, \text{ and } 117.1 \text{ kHz})$, respectively. Error bars represent the Bayesian 90% credible interval for the visibility. While the traces are very similar, increasing the number of ions tends to produce sharper features.

in which $\mathbf{x}_1(t) = U_{\text{free}}(t)^\dagger \mathbf{x}_1 U_{\text{free}}(t)$, where \mathbf{x}_1 is the position operator of the first ion, \mathbf{k}_L is the wavevector of the laser, Ω_0 is the Rabi frequency of the driving laser with frequency $\omega_L = \omega_0 + \Delta$ and phase ϕ . Here, Δ is chosen as the frequency of radial oscillations of the first ion along the direction of \mathbf{k}_L .

The ion chain is cooled to the Doppler limit to a mean phonon occupation number of $\bar{n} \approx 5$. With a Lamb-Dicke parameter of $\eta \approx 0.05$, we obtain $\eta \sqrt{\bar{n}} \approx 0.11 \ll 1$, hence, we can approximate the Hamiltonian further by assuming the Lamb-Dicke regime². Moreover, we apply a rotating-wave approximation (discarding fast-rotating terms that contain the operators $a_1^\dagger \sigma_+$ and $a_1 \sigma_-$) to finally obtain the unitary operator describing the action of the first Ramsey pulse

$$R(\theta, \phi) = \exp \left\{ \frac{\theta}{2} \left(e^{i\phi} \sigma_+ a_1^\dagger - e^{-i\phi} \sigma_- a_1 \right) \right\}, \quad (12)$$

in which $\theta = \eta \Omega_0 \tau$ and τ denotes the pulse duration.

D. Time-evolution under the Ramsey pulse sequence

Let us now describe the evolution of the initial quantum state ρ_{in} under the Ramsey sequence. We first focus on the description of the quantum state after an initial sideband pulse with phase ϕ_1 , followed by free evolution for a time t , which leads to the following quantum state:

$$\rho(\theta, \phi_1; t) = U_{\text{free}}(t)R(\theta, \phi_1)\rho_{\text{in}}R^\dagger(\theta, \phi_1)U_{\text{free}}^\dagger(t). \quad (13)$$

The free evolution is described by $U_{\text{free}}(t) = \exp(-iH_{\text{free}}t)$, where H_{free} was introduced in Eq. (6). Since $[H_{\text{free}}, \rho_{\text{in}}] = 0$, we can rewrite the above expression as

$$\rho(\theta, \phi_1; t) = R(\theta, \phi_1; -t)\rho_{\text{in}}R^\dagger(\theta, \phi_1, -t), \quad (14)$$

where $R(\theta, \phi_i; -t) = U_{\text{free}}(t)R(\theta, \phi_i)U_{\text{free}}^\dagger(t)$. We further express $R(\theta, \phi; -t)$ in terms of collective modes,

$$\begin{aligned} R(\theta, \phi; -t) &= \exp\left(-i\sum_{i=1}^N\omega_iA_i^\dagger A_i t\right)\exp\left\{\frac{\theta}{2}\left(e^{i(\phi-\omega_0 t)}\sigma_+ \sum_{j=1}^N\beta_{1j}^*A_j^\dagger - e^{-i(\phi-\omega_0 t)}\sigma_- \sum_{j=1}^N\beta_{1j}A_j\right)\right\} \\ &\quad \times \exp\left(i\sum_{i=1}^N\omega_iA_i^\dagger A_i t\right). \end{aligned}$$

The bosonic commutation relations of the collective mode operators lead to interaction-picture operators of the form $e^{-i\omega_j A_j^\dagger A_j t} f(A_j^\dagger, A_j) e^{i\omega_j A_j^\dagger A_j t} = f(A_j^\dagger e^{-i\omega_j t}, A_j e^{i\omega_j t})$, where $f(A_j^\dagger, A_j)$ is some function of the collective mode operators A_j^\dagger and A_j . We write

$$R(\theta, \phi; -t) = \exp\left(\frac{\theta}{2}u(\phi, -t)\right), \quad (15)$$

where $u(\phi, -t) = e^{i(\phi-\omega_0 t)}\sigma_+ A(t)^\dagger - e^{-i(\phi-\omega_0 t)}\sigma_- A(t)$. We have further introduced

$$A^\dagger(t) = a_1^\dagger(-t) = \sum_{j=1}^N\beta_{1j}^*A_j^\dagger e^{-i\omega_j t} = \sum_{k=1}^N\gamma_k(t)a_k^\dagger, \quad (16)$$

with

$$\gamma_k(t) = \sum_{j=1}^N\beta_{1j}^*\beta_{kj}e^{-i\omega_j t}. \quad (17)$$

Finally, after application of the second Ramsey pulse (with phase ϕ_2 and same duration $\theta/2$ as the first one), the density matrix is given by

$$\begin{aligned} \rho_f(\theta, \phi_1, \phi_2; t) &= R(\theta, \phi_2; 0)\rho(\theta, \phi_1; t)R^\dagger(\theta, \phi_2; 0), \\ &= R(\theta, \phi_2; 0)R(\theta, \phi_1; -t)\rho_{\text{in}}R^\dagger(\theta, \phi_1; -t)R^\dagger(\theta, \phi_2; 0). \end{aligned} \quad (18)$$

E. Visibility

In the experiment, we measure the population of the $|D\rangle$ state, which is given by

$$P_D(\theta, \phi_1, \phi_2; t) = \text{tr}[P_D \rho(\theta, \phi_1, \phi_2; t)], \quad (19)$$

where tr denotes the trace, $P_D = |D\rangle\langle D| \otimes \mathbb{I}_N$, and \mathbb{I}_N is the identity operator on the Fock space of the N bosonic modes. With the final state $\rho_f(\theta, \phi_1, \phi_2; t)$, as defined in Eq. (18), we obtain

$$P_D(\theta, \phi_1, \phi_2; t) = \text{tr}\left[P_D \exp\left(\frac{\theta}{2}u(\phi_2, 0)\right) \exp\left(\frac{\theta}{2}u(\phi_1, -t)\right) \rho_{\text{in}} \exp\left(-\frac{\theta}{2}u(\phi_1, -t)\right) \exp\left(-\frac{\theta}{2}u(\phi_2, 0)\right)\right]. \quad (20)$$

This result is valid in the Lamb-Dicke regime for arbitrary pulse duration $\theta/2$. To find an analytical expression for the Ramsey fringe visibility we approximate this expression further, based on experimentally motivated assumptions.

In the experiment, the normal mode frequencies are of the order of $\omega_j \approx 2\pi \times 2$ MHz, while the spread of normal modes is given by $\Delta\omega \lesssim 2\pi \times 100$ kHz. Therefore, $\Delta\omega/\omega_j \approx 0.05$, which implies that the average number of phonons in normal modes $\bar{n}_j = \langle A_j^\dagger A_j \rangle_{\rho_{\text{ph}}} = \text{tr}\{A_j^\dagger A_j \rho_{\text{ph}}\}$ are approximately equal. Hence, we assume that the initial state describes an incoherent, homogeneous phonon distribution among the collective modes, i.e.,

$$\langle A_j^\dagger A_k \rangle_{\rho_{\text{ph}}} \approx \bar{n} \delta_{jk}. \quad (21)$$

Furthermore, we expand $R(\theta, \phi; -t)$ up to second order in the pulse duration $\theta/2$. In all of our measurements, $\theta/2 \lesssim 0.32$. We obtain

$$P_D(\theta, \phi_1, \phi_2; t) = \left(\frac{\theta}{2}\right)^2 (\bar{n} + 1) \sum_{j,k,l=1}^N \left(e^{i\phi_2} \gamma_j(t) + e^{i\phi_1} \delta_{j1}\right) \left(e^{-i\phi_2} \gamma_j^*(t) + e^{-i\phi_1} \delta_{j1}\right) \beta_{jk}^* \beta_{lk} + \mathcal{O}(\theta^4), \quad (22)$$

where \bar{n} is the average phonon occupation number per normal modes. Using $\sum_{j=1}^N |\gamma_j(t)|^2 = 1$ and $\Delta\phi = \phi_1 - \phi_2$, the expression above can be simplified to

$$P_D(\theta, \phi_1, \phi_2; t) = \left(\frac{\theta}{2}\right)^2 (\bar{n} + 1) \left(2 + e^{-i(\Delta\phi)} \gamma_1(t) + e^{i(\Delta\phi)} \gamma_1^*(t)\right) + \mathcal{O}(\theta^4). \quad (23)$$

The fringe visibility is now given by

$$v(t) = \frac{\max(P_D(t)) - \min(P_D(t))}{\max(P_D(t)) + \min(P_D(t))} \approx |\gamma_1(t)|, \quad (24)$$

where the maximum and minimum are taken by optimizing over the phase difference $\Delta\phi$ between the two Ramsey pulses. The final result is obtained by writing $\gamma_1(t) = |\gamma_1(t)|e^{i\varphi(t)}$ and realizing that $\max(P_D(t))$ and $\min(P_D(t))$ are attained at $\Delta\phi = \varphi(t)$ and $\Delta\phi = \varphi(t) + \pi$, respectively. The function $\gamma_1(t)$ was introduced in Eq. (17). The result (24) was used to predict the time evolution of the visibility in Figures 3 and 4 of the main manuscript.

SUPPLEMENTARY NOTE 2. TWO-POINT CORRELATION FUNCTION

The above Ramsey scheme can be interpreted as a method to extract the two-point auto-correlation function of the phonons by means of spin measurements. To see this, consider the first ion's phonon annihilation operator in the Heisenberg picture, which using Eq. (8) reads,

$$a_1(t) = e^{+iH_{\text{free}}t} a_1 e^{-iH_{\text{free}}t} = \sum_j \beta_{1j} A_j e^{-i\omega_j t}. \quad (25)$$

With this, the two-point auto-correlation function of the phonons is given by

$$\langle a_1(t) a_1^\dagger(0) \rangle = \sum_{jk} \beta_{1j} \beta_{1k}^* e^{-i\omega_j t} \langle A_j A_k^\dagger \rangle. \quad (26)$$

With the assumption of an initial phonon state that is diagonal in the collective mode basis, and whose population is independent of the mode index j , c.f. Eq. (21), we obtain

$$\begin{aligned} \langle a_1(t) a_1^\dagger(0) \rangle &= \sum_j \beta_{1j} \beta_{1j}^* e^{-i\omega_j t} \langle A_j A_j^\dagger \rangle \\ &= (\bar{n} + 1) \gamma_1(t), \end{aligned} \quad (27)$$

where, again, $\bar{n} = \langle A_j^\dagger A_j \rangle$. Thus, the experimental scheme may be seen as a local method to directly determine the modulus of the two-point correlations functions of the phonon chain.

Based on this argument, we expect that suitable extensions of the scheme to protocols consisting of more than two pulses are in fact capable of extracting also higher-order phonon auto-correlation functions. This way, the methods of non-linear spectroscopy, which are typically employed to study dynamical and spectral features of molecular aggregates and semiconductors², become accessible to probe this many-body system. This opens up a powerful way of analyzing complex interacting quantum systems, especially if combined with the single-site addressability that is unique to quantum optical systems⁴⁻⁷.

SUPPLEMENTARY NOTE 3. MONITORING OF SPIN-PHONON DISCORD DYNAMICS

In this section, we show that the Ramsey signal discussed above reveals the dynamics of discord-type correlations between the electronic and motional degree of freedom of the first ion. To this end, we revisit the density matrix $\rho(\theta, \phi_1; t)$ of the total system after the first sideband pulse and after free evolution of the chain (duration t), which was previously introduced in Eq. (14). Within second order

in $\theta/2$ the density matrix is given by

$$\begin{aligned} \rho(\theta, \phi_1; t) = & |0\rangle\langle 0| \otimes \left[\rho_{\text{ph}} - \frac{\theta^2}{8} \left(A(t)A^\dagger(t)\rho_{\text{ph}}^{(1)} + \rho_{\text{ph}}A(t)A^\dagger(t) \right) \right] \\ & + |1\rangle\langle 1| \otimes \frac{\theta^2}{4} A^\dagger(t)\rho_{\text{ph}}A(t) \\ & + \frac{\theta}{2} \left(|1\rangle\langle 0| \otimes e^{i\phi_1} A^\dagger(t)\rho_{\text{ph}} + |0\rangle\langle 1| \otimes e^{-i\phi_1} \rho_{\text{ph}}A(t) \right). \end{aligned} \quad (28)$$

where $A(t)$ was introduced in Eq. (16). Taking the trace over the local phonons $i = 2, \dots, N$ one finds the density matrix describing the combined quantum state of the electronic and the motional degrees of freedom of the first ion:

$$\begin{aligned} \rho^{(1)}(t, \tau_1, \phi_1) = & \text{tr}_{[2,N]} \rho(t, \tau_1, \phi_1) \\ = & |0\rangle\langle 0| \otimes Y(t) + |1\rangle\langle 1| \otimes Z(t) \\ & + \frac{\theta}{2} \left(|1\rangle\langle 0| \otimes e^{i\phi_1} \gamma_1(t) a_1^\dagger \rho_{\text{ph}}^{(1)} + |0\rangle\langle 1| \otimes e^{-i\phi_1} \gamma_1^*(t) \rho_{\text{ph}}^{(1)} a_1 \right). \end{aligned} \quad (29)$$

Here, $\rho_{\text{ph}}^{(1)} = \text{tr}_{[2,N]} \rho_{\text{ph}}$ is the reduced state of the motional degree of freedom of the first ion, while $Y(t)$ and $Z(t)$ are certain operators acting on the corresponding state space. In order to derive (29) from (28) we have used the relation $\text{tr}_{[2,N]} \{ \rho_{\text{ph}} a_k \} = \delta_{k1} \rho_{\text{ph}}^{(1)} a_1$.

With the help of expression (29) we can easily determine the quantum discord between the electronic and the motional degrees of freedom of the first ion. A simple way to estimate the discord-type correlations is obtained from the dephasing-induced disturbance⁸⁻¹⁰, given by

$$D(t) = \frac{1}{2} \|\rho^{(1)}(t, \tau_1, \phi_1) - \rho_{\text{deph}}^{(1)}(t, \tau_1, \phi_1)\|, \quad (30)$$

where $\|\cdot\|$ denotes the trace norm and $\rho_{\text{deph}}^{(1)}(t, \tau_1, \phi_1)$ is the state obtained from the state $\rho^{(1)}(t, \tau_1, \phi_1)$ after dephasing in its eigenbasis:

$$\rho_{\text{deph}}^{(1)}(t, \tau_1, \phi_1) = |0\rangle\langle 0| \otimes Y(t) + |1\rangle\langle 1| \otimes Z(t). \quad (31)$$

Thus, we have $D(t) = \frac{1}{2} \|X(t)\|$, where

$$\begin{aligned} X(t) \equiv & \rho^{(1)}(t, \tau_1, \phi_1) - \rho_{\text{deph}}^{(1)}(t, \tau_1, \phi_1) \\ = & \frac{\theta}{2} \left(|1\rangle\langle 0| \otimes e^{i\phi_1} \gamma_1(t) a_1^\dagger \rho_{\text{ph}}^{(1)} + |0\rangle\langle 1| \otimes e^{-i\phi_1} \gamma_1^*(t) \rho_{\text{ph}}^{(1)} a_1 \right). \end{aligned}$$

To evaluate this expression analytically, we realize another approximation. In particular, we consider the local phonon state to be of the form

$$\rho_{\text{ph}}^{(1)} = \sum_{n_1=0}^{\infty} p_{n_1} |n_1\rangle\langle n_1|. \quad (32)$$

A detailed discussion of this approximation will be given at the end of this section. Using this, one finds that the eigenvalues of $X(t)$ are given by

$$\pm \frac{\theta}{2} |\gamma_1(t)| p_{n_1} \sqrt{n_1 + 1}, \quad n_1 = 0, 1, 2, \dots, \quad (33)$$

which yields:

$$\begin{aligned} D(t) &= \frac{1}{2} \|X(t)\| = \sum_{n_1=0}^{\infty} \frac{\theta}{2} |\gamma_1(t)| p_{n_1} \sqrt{n_1 + 1} \\ &= \frac{\theta}{2} \langle \sqrt{n_1 + 1} \rangle |\gamma_1(t)|. \end{aligned} \quad (34)$$

This shows that the discord-type quantum correlations of the degrees of freedom of the first ion are proportional to the visibility $|\gamma_1(t)|$. The decay and revival of the visibility observed in the experiment thus correspond to a loss and gain of the quantum correlations between the electronic and motional degrees of freedom of the first ion of the chain.

We can further combine Eqs. (27) and (34), leading to:

$$D(t) = \frac{\theta}{2} \frac{\langle \sqrt{n_1 + 1} \rangle}{\bar{n} + 1} \left| \langle a_1(t) a_1^\dagger(0) \rangle \right| \approx \frac{\theta}{2} \frac{\left| \langle a_1(t) a_1^\dagger(0) \rangle \right|}{\sqrt{\bar{n} + 1}}. \quad (35)$$

The measure of discord-type quantum correlations is thus directly proportional to the modulus of the two-point correlation function of the motional amplitude of the first ion. This result is valid for perturbatively small values of $\frac{\theta}{2}$. For the special case of $\pi/2$ pulses as applies to present experiments,

$$D(t) \approx \frac{\pi}{4} \frac{\left| \langle a_1(t) a_1^\dagger(0) \rangle \right|}{\bar{n} + 1}, \quad (36)$$

in which we replaced $\theta \langle \sqrt{n + 1} \rangle$ with $\pi/2$ indicating a Ramsey $\pi/2$ -pulse from equation (12). In this case, the perturbation parameter is $\frac{\theta}{2} \approx 0.3$. The equation above leads to

$$D(t) \approx \frac{\pi}{4} v(t), \quad (37)$$

which indicates a direct proportionality between discord and visibility, and thereby proves visibility as a quantitative measure for discord-type quantum correlations in the chain.

To determine the coherences and the discord of the state of the electronic and the motional degrees of freedom of the first ion we have used the additional assumption that the phonon state (10) may be replaced by an equilibrium state of the local modes a_j :

$$\rho_{\text{ph}}^a = \frac{1}{Z_a} \exp \left[-\beta \sum_j \hbar \omega_j a_j^\dagger a_j \right]. \quad (38)$$

Averages taken with ρ_{ph}^A are denoted by $\langle \dots \rangle_A$ and averages with ρ_{ph}^a are denoted by $\langle \dots \rangle_a$. To justify the replacement $\rho_{\text{ph}}^A \rightarrow \rho_{\text{ph}}^a$ we require that all first and second moments of A_j determined by ρ_{ph}^A and ρ_{ph}^a are identical. It is clear that we have the following exact relations:

$$\langle A_i \rangle_A = \langle A_i \rangle_a = 0, \quad (39)$$

$$\langle A_i A_j \rangle_A = \langle A_i A_j \rangle_a = 0. \quad (40)$$

Thus, we only have to demand that also

$$\langle A_i^\dagger A_j \rangle_A = \langle A_i^\dagger A_j \rangle_a \quad (41)$$

holds, which yields the condition

$$\delta_{ij} \bar{n}_j = \sum_k \beta_{ki} \beta_{kj}^* \bar{n}_k. \quad (42)$$

By condition (21) this becomes

$$\delta_{ij} \bar{n} = \sum_k \beta_{ki} \beta_{kj}^* \bar{n}, \quad (43)$$

which is obviously satisfied since the matrix (β_{ij}) is unitary.

SUPPLEMENTARY REFERENCES

* Corresponding author: mabd@kth.se

† Corresponding author: hhaeffner@berkeley.edu

¹ Morigi, G. & Eschner, J. Is an ion string laser-cooled like a single ion? *J. Phys. B* **36**, 1041 (2003).

² Leibfried, D., Blatt, R., Monroe, C. & Wineland, D. Quantum dynamics of single trapped ions. *Reviews of Modern Physics* **75**, 281–324 (2003).

³ Mukamel, S. Principles of Nonlinear Optics and Spectroscopy. *Oxford Univ. Press, New York* (1995).

⁴ Gessner, M., Schlawin, F., Häffner, H., Mukamel, S. & Buchleitner, A. Nonlinear spectroscopy of controllable many-body quantum systems. *New Journal of Physics* **16** 092001 (2014).

⁵ Schlawin, F., Gessner, M., Mukamel, S. & Buchleitner, A. Nonlinear spectroscopy of trapped ions. *Physical Review A* **90**, 023603 (2014).

⁶ Gessner, M., Schlawin, F., & Buchleitner, A. Probing polariton dynamics in trapped ions with phase-coherent two-dimensional spectroscopy. *Chem. Phys.* **142**, 212439 (2015).

⁷ Lemmer, A., Cormick, C, Schmiegelow, C.T., Schmidt-Kaler, F., & Plenio, M. B. Two-Dimensional Spectroscopy for the Study of Ion Coulomb Crystals. *Phys. Rev. Lett.* **114**, 073001 (2015).

- ⁸ Gessner, M. & Breuer, H.-P. Detecting Nonclassical System-Environment Correlations by Local Operations. *Phys. Rev. Lett.* **107**, 180402 (2011).
- ⁹ Gessner, M. & Breuer, H.-P. Local witness for bipartite quantum discord. *Phys. Rev. A* **87**, 042107 (2013).
- ¹⁰ Gessner, M. Dynamics and Characterization of Composite Quantum Systems. *PhD Thesis, Albert-Ludwigs-Universität Freiburg*, (2015).